Helicons and Nonresonant Cyclotron Absorption in Semiconductors. I. InSb†‡

JOHN D. WILEY,* P. S. PEERCY,§ and R. N. DEXTER
Department of Physics, University of Wisconsin, Madison, Wisconsin 53706
(Received 25 September 1968)

We describe techniques of experiment and analysis for using microwave helicon interferometry and nonresonant cyclotron absorption to determine the carrier densities, effective masses, mobilities, and lattice dielectric constants for certain semiconductors and semimetals. InSb was used as an example and as a test of the applicability of our techniques. Circularly polarized microwaves of frequencies 24 and 70 GHz and magnetic fields up to 1.9 Wb/m^2 were used in reflection and transmission experiments at temperatures between 1.3°K and room temperature. The primary studies were made at 77°K on single crystals of n-type InSb which ranged in electron concentration from 8×10^{19} to 7×10^{22}m^{-3}. For these samples we obtained $m^*=0.014m_0$ and $\epsilon_L=19.7\epsilon_0$. Studies of the change in carrier concentration with temperature gave a value of 0.26 eV for the band gap. All of these numbers are in good agreement with literature values and confirm the utility of the techniques which were subsequently used to study gray tin and $Hg_{1-x}Cd_xTe$.

I. INTRODUCTION

MAGNETOPLASMA propagation in metals similar to whistler propagation in the ionosphere was first discussed by Konstantinov and Perel,[1] and independently Aigrain[2] showed that these magnetoplasma waves could be transmitted through semiconductors. This propagation occurs when the solid is immersed in a dc magnetic field with an incident electromagnetic wave of frequency ω such that the conditions $\omega_c\tau\gg1$ and $\omega_c>\omega$ are satisfied for at least one type of charge carrier. ω_c is the cyclotron frequency of the charge carrier, $\omega_c=eB/m^*$, and τ is its scattering time. Under the condition $\omega_c\tau\gg1$, the charge carriers can perform an orbit about the dc magnetic field many times between collisions. A circularly polarized electromagnetic wave can then propagate with low attenuation and low velocity parallel to the magnetic field, provided that the frequency of the wave is less than the cyclotron frequency and the rotation of the wave is in the same sense as the rotation of the charge carriers. Since the initial proposals, such transmission has been observed in metals, semimetals, and semiconductors. The electromagnetic waves are known as helicon waves in media which contain only one type of charge carrier and Alfven waves in media where both electrons and holes participate in the propagation. Alfven-wave propagation has been observed in several semimetals[3–8] and should occur in intrinsic semiconductors when the conditions $\omega_c\tau\gg1$ and $\omega_c\gg\omega$ are satisfied by both electrons and holes. The wave is heavily damped, however, unless $\omega\tau>1$. In our experiments this propagation mode is not observed.

Helicon propagation was first reported by Bowers, Legendy, and Rose[9] in sodium at audio frequencies. Similar experiments in many metals have since been reported.[10–17] Experimental and theoretical investigations have been made in metals for Doppler-shifted cyclotron resonance and other nonlocal effects[15,18–23] and for the interaction of helicons with phonons,[24–27] magnons,[28,29] and drift currents.[30] The propagation of

† Sponsored by the Aerospace Research Laboratories, Office of Aerospace Research, U. S. Air Force.

‡ This paper is based on portions of theses submitted by J. D. W. and P. S. P. in partial fulfillment of the requirements for the Ph.D. degree at the University of Wisconsin.

* Present address: Bell Telephone Laboratories, Murray Hill, N. J.

§ Present address: The Sandia Corporation, Albuquerque, N. M.

[1] O. V. Konstantinov and V. I. Perel, Zh. Eksperim. i Teor. Fiz. **38**, 161 (1960) [English transl.: Soviet Phys.—JETP **11**, 117 (1960)].

[2] P. Aigrain, in *Proceedings of the International Conference on Semiconductor Physics, Prague, 1960* (Academic Press Inc., New York, 1961), p. 224.

[3] M. Surma, J. K. Furdyna, and H. C. Praddaude, Phys. Rev. Letters **13**, 710 (1964).

[4] G. A. Williams, Bull. Am. Phys. Soc. **9**, 353 (1963).

[5] G. A. Williams and G. E. Smith, IBM J. Res. Develop. **8**, 276 (1964); G. A. Williams, Phys. Rev. **139**, A771 (1965).

[6] S. J. Buchsbaum and J. K. Galt, Phys. Fluids **4**, 1514 (1961).

[7] J. Kirsch, Phys. Rev. **133**, A1390 (1964).

[8] D. J. Bartelink and W. A. Norland, Phys. Rev. **152**, 556 (1966).

[9] R. Bowers, C. R. Legendy, and F. E. Rose, Phys. Rev. Letters **7**, 339 (1961).

[10] P. Cotti, A. Quattropani, and P. Wyder, Physik Kondensierten Materie **1**, 27 (1963).

[11] P. Cotti, P. Wyder, and A. Quattropani, Phys. Letters **1**, 50 (1962).

[12] R. G. Chambers and B. K. Jones, Proc. Roy. Soc. (London) **A270**, 417 (1962).

[13] M. T. Taylor, J. R. Merrill, and R. Bowers, Phys. Rev. **129**, 2525 (1963).

[14] J. R. Merrill, M. T. Taylor, and J. M. Goodman, Phys. Rev. **131**, 2499 (1963).

[15] M. T. Taylor, J. R. Merrill, and R. Bowers, Phys. Letters **6**, 159 (1963).

[16] C. C. Grimes, in *Proceeding of the Seventh International Conference on the Physics of Semiconductors, Paris, 1964*, edited by M. Hulin (Academic Press Inc., New York, 1969), Vol. I, p. 87.

[17] W. F. Druyvesteyn, G. J. van Gusp, and C. A. A. J. Greebe, Phys. Letters **22**, 248 (1966).

[18] E. A. Stern, Phys. Rev. Letters **10**, 91 (1961).

[19] M. T. Taylor, Phys. Rev. Letters **12**, 497 (1964).

[20] M. T. Taylor, Phys. Rev. **137**, A1145 (1965).

[21] A. W. Overhauser and S. Rodriguez, Phys. Rev. **141**, 431 (1966).

[22] J. C. McGroddy, J. L. Stanford, and E. A. Stern, Phys. Rev. **141**, 437 (1966).

[23] J. L. Stanford and E. A. Stern, Phys. Rev. **144**, 534 (1966).

[24] D. N. Langenburg and J. Bok, Phys. Rev. Letters **11**, 549 (1963).

[25] J. J. Quinn and S. Rodriguez, Phys. Rev. Letters **11**, 552 (1963).

[26] C. C. Grimes and S. J. Buchsbaum, Phys. Rev. Letters **12**, 357 (1964).

[27] J. J. Quinn and S. Rodriguez, Phys. Rev. **133**, A1589 (1964).

[28] E. A. Stern and E. R. Callen, Phys. Rev. **131**, 512 (1963).

[29] C. C. Grimes (private communication).

[30] D. J. Bartelink, Phys. Rev. Letters **12**, 479 (1964).

helicons in metals has also been used for Fermi-surface studies and model testing.[18–23,31–33]

Helicon propagation occurs in intrinsic and extrinsic semiconductors when the condition $\omega_c\tau \gg 1$ is satisfied for only one type of charge carrier. This propagation has been observed in PbTe and HgSe at radio frequencies[34–37] and in InAs,[38,39] PbTe,[40] HgTe,[41] IbSn,[12,38,39,41–46] α-Sn[42,46], Ge[39], and $Hg_{1-x}Cd_xTe$[47] at microwave frequencies. These studies of helicons and their uses in probing solids have been reviewed by several authors.[48–50] Thus, the theory and practice of helicon propagation are well established and understood. Nevertheless, the primary use of this technique in semiconductors has been for measurements of the free-carrier concentration.

The intention of the work reported here was to learn how to exploit these phenomena for a practical determination of the parameters m^*, μ, and ϵ_L of a semiconductor, as well as the carrier concentration N. For this reason we decided to reinvestigate InSb, where the electron effective mass and dielectric constant are well known. The present study was undertaken in a low magnetic field range where the conditions $\omega_c \gg \omega$ and $\omega_c\tau \gg 1$ begin to break down, necessitating consideration of more terms than are customarily retained in the expansion for the refractive index of the medium. Measurement of these additional terms in the refractive index can provide an accurate measurement of the effective mass of the charge carrier supporting the helicon mode of propagation.

Most of our measurements were performed using Fabry-Perot interferometry and cavity techniques, monitoring the reflected signal as a function of magnetic field. This technique was chosen for two reasons. In the region of high attenuation encountered at low magnetic fields only a very small signal is transmitted. For accurate measurements of the electronic effective mass it was therefore advantageous to detect the reflected signal that allows good resolution of the interference effects. The method of Rayleigh interferometry[44] also gives high resolution but the presence of an arbitrary phase term is troublesome for effective-mass analysis. Secondly, as will be shown in Sec. II, the derivative of the reflected signal has a sharp maximum at low fields. We will show how this inflection point of the nonresonant cyclotron absorption (NRCA) may be used to measure the mobility and effective mass.

We believe that the central contribution of this paper is to demonstrate how the combination of helicon propagation and NRCA permits a rapid and partially redundant, electrodeless determination of the carrier density, effective mass, and mobility in certain classes of semiconductors.

The theory of helicon interferometry in thin slabs is presented in Sec. II A. In Sec. II B we describe a technique (which we call the "inflection point" technique) for utilizing NRCA to obtain effective masses and mobilities. The utilization of the amplitude envelope of the helicon interference fringes to obtain mobilities is discussed in Sec. II C. Section III contains a discussion of experimental techniques. In Sec. IV we present the analysis of experimental data. The major results of our work are summarized in Sec. V.

II. THEORETICAL

A. Helicon Interferometry

The theory of helicon propagation in semiconductors was first discussed by Aigrain.[2] Other authors[51–55] have also given theoretical treatments obtaining both the index of refraction of the medium under the influence of a magnetic field and the various modes of propagation which arise from different boundary conditions. The approximations made in earlier analyses emphasize the determination of the carrier concentration of the medium by means of helicon propagation. Here we will emphasize the special considerations relating to the determination of parameters other than the carrier concentration.

The analysis will be based on the simplest possible theoretical model. For the semiconductor we will assume a single mobile carrier type with isotropic mass and scattering time. We assume that circularly polarized

[31] C. C. Grimes, G. Adams, and P. H. Schmidt, Phys. Rev. Letters **15**, 409 (1965).
[32] A. L. McWhorter and J. N. Walpole, Phys. Rev. **163**, 618 (1967).
[33] P. A. Penz, Phys. Rev. Letters **20**, 725 (1968).
[34] Y. Kanai, Japan. J. Appl. Phys. **1**, 132 (1962); in *Proceedings of the Seventh International Conference on the Physics of Semiconductors*, edited by M. Hulin (Academic Press Inc., New York, 1964), Vol. I., p. 45.
[35] C. Nanney, Phys. Rev. **138**, A1484 (1965).
[36] W. Schilz, Solid State Commun. **5**, 503 (1967).
[37] H. Gobrecht, A. Tausend, and J. Danckwerts, Solid State Commun. **5**, 551 (1967).
[38] J. K. Furdyna, Phys. Rev. Letters **16**, 646 (1966).
[39] J. K. Furdyna, Rev. Sci. Instr. **37**, 462 (1966).
[40] J. N. Walpole and A. L. McWhorter, Phys. Rev. **158**, 708 (1967).
[41] J. P. Jamet, B. Lemaire, V. Cagan, and C. Verie, J. Phys. Soc. Japan, Suppl. **21**, 718 (1966).
[42] D. H. Hensler, thesis, University of Wisconsin, 1962 (unpublished).
[43] A. Libchaber and R. Veilex, Phys. Rev. **127**, 774 (1962).
[44] J. K. Furdyna, Appl. Opt. **6**, 675 (1967).
[45] B. E. Burke and G. S. Kino, J. Appl. Phys. **38**, 4888 (1968).
[46] P. S. Peercy and R. N. Dexter, Bull. Am. Phys. Soc. **10**, 385 (1965); P. S. Peercy, R. N. Dexter, and A. W. Ewald, Bull. Am. Phys. Soc. **10**, 1090 (1965).
[47] J. D. Wiley and R. N. Dexter, Bull. Am. Phys. Soc. **13**, 94 (1968); J. D. Wiley and R. N. Dexter, following paper, Phys. Rev. **181**, 1181 (1969).
[48] R. Bowers and M. C. Steele, Proc. IEEE **52**, 1105 (1964).
[49] A. G. Chynoweth and S. J. Buchsbaum, Phys. Today **18**, 26 (1965).
[50] D. P. Morgan, Phys. Status Solidi **24**, 9 (1967).
[51] C. R. Legendy, Phys. Rev. **135**, A1713 (1964).
[52] G. N. Harding and P. C. Thonemann, Proc. Phys. Soc. (London) **85**, 317 (1965).
[53] R. Hirota, J. Phys. Soc. Japan **19**, 1130 (1964).
[54] E. A. Kaner and V. G. Skobov, Zh. Eksperim. i Teor. Fiz. **45**, 610 (1963) [English transl.: Soviet Phys.—JETP **18**, 419 (1964)].
[55] J. P. Klozenberg, B. McNamara, and P. C. Thonemann, J. Fluid Mech. **21**, 545 (1965).

microwaves are propagating along the dc magnetic field and we restrict ourselves to the local limit—$ql \ll 1$, where q is the wave vector and l is the electronic mean free path. Other authors[32,50] have shown how some or all of these restrictions can be removed, but the simpler model is quite adequate for the description of helicon propagation in a wide range of III-V and II-VI semiconductors, and it was the possibility of using helicons to study these materials which motivated this work.

Under the above assumptions, the complex index of refraction is given in rationalized MKS units by

$$(n_\pm - ik_\pm)^2 = \frac{\epsilon_L}{\epsilon_0} - \frac{iNe^2\tau}{\epsilon_0 \omega m^*[1+i(\omega \pm \omega_c)\tau]}, \quad (1)$$

where the permeability of the medium has been taken to be that of free space and the + and − signs denote the two directions of circular polarization for a fixed direction of B or the opposing directions of B for a fixed sense of polarization. ϵ_L denotes the permittivity of the lattice, N the carrier concentration, τ the scattering time, and e the magnitude of the electronic charge.

The limit of interest for analysis of the helicon data taken in InSb at microwave frequencies and low magnetic fields is $\omega_c^2\tau^2 \gg 1$ and $\omega_c > \omega$. The free carriers in this case are electrons. Furdyna[56] has shown that, as long as $\omega_{ch}\tau_h \ll 1$, the only effect of the holes is an additional damping of the helicon waves. For all data taken at 77°K

$$N_h \ll N_e \quad \text{and} \quad \omega_{ch}\tau_h \ll 1,$$

so that all contributions due to the holes can be neglected. In this limit the real and imaginary parts of the index of refraction are readily obtained.

Henceforth, the following conventions will be adopted: e and ω_c will be taken to be positive quantities, so that for a given circular polarization the orientation of the dc magnetic field which would show cyclotron resonance will be called the minus orientation and corresponds to the minus sign in Eq. (1). Following Furdyna,[44] we will refer to this as the CRA (cyclotron-resonance-active) side of the magnetic field. The plus orientation of the field will be denoted CRI (cyclotron-resonance-inactive).

Restricting our attention to the CRA side of magnetic field, n_-^2 and k_-^2 can be expanded in a power series in $1/B$ or $1/\omega_c$. When this is done one obtains

$$n_-^2 \approx \frac{\epsilon_L}{\epsilon_0} + \frac{\omega_p^2}{\omega\omega_c}\left[1 + \frac{\omega}{\omega_c} + \frac{\omega^2}{\omega_c^2}\left(1 - \frac{3}{4\omega^2\tau^2}\right) + \cdots\right] \quad (2)$$

and

$$k_-^2 \approx (\omega_p^2/\omega\omega_c)[(4\omega_c^2\tau^2)^{-1} + \cdots], \quad (3)$$

where $\omega_p = (Ne^2/\epsilon_0 m^*)^{1/2}$.

It is impracticable to obtain a unique 4-parameter fit of N, m^*, ϵ_L, and τ to the experimental helicon data for

[56] J. K. Furdyna, Phys. Rev. Letters **14**, 635 (1965).

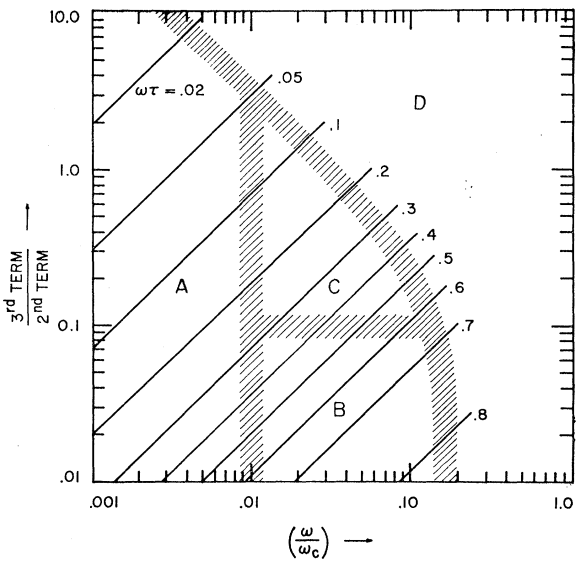

FIG. 1. Diagram for determining the number of terms which must be retained in the expansion for n_-^2 (Eq. 2) as described in the text.

n_-^2 and it is therefore imperative to work in a regime in which the third $(1/\omega_c^3)$ term is negligible. It is convenient to distinguish several experimental regimes. Figure 1 shows the ratio of the third term of Eq. (2) to the second term plotted versus ω/ω_c (which is the ratio of the second term to the first term). In region A it is seen that $\omega/\omega_c < 0.01$, so that the terms higher than the first make a total contribution of a few percent or less, depending on $\omega\tau$. This is the region that is usually referred to as the "classical helicon approximation." In this approximation $n_-^2 \propto 1/B$. In region B the ratio of the third to the second term is <0.1, so that one can hope to omit the third term in the expansion. Note that one needs $\omega\tau \gtrsim 0.4$ in order to enter this regime where the second term makes a 1–10% contribution and provides a means of measuring m^*. In region C all three terms must be retained and the expression for n_-^2 becomes unwieldy. Finally, in region D no helicon propagation is observed. The curved gray boundary corresponds to $\omega_c\tau = \mu B = 5$ and should be considered to be only a rough indicator of the lowest field at which helicon effects will be observed.

The magnetic field dependence of the index of refraction on the CRA side can now be used as follows. If one assumes normal incidence of the microwaves on a thin sample of thickness L, the condition for reflection minima, or transmission maxima, is simply

$$L = M\lambda_0/2n_-, \quad M = 1, 2, 3, \cdots \quad (4)$$

where λ_0 is the wavelength of the microwaves in free space.

In cases where the lateral dimensions of the sample are not large compared with the thickness, the resonance condition is modified. This problem has been dealt with

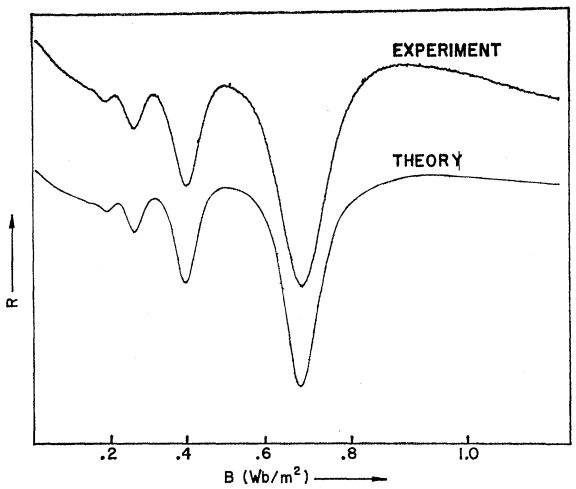

FIG. 2. A comparison of an experimental trace with the results of a calculation using Eq. (1) and the theoretical reflection coefficient. Numbers used in the theoretical expression were obtained experimentally by methods described in the text. The curves are displaced vertically for clarity.

empirically[19,57] and theoretically.[12,51] In all cases reported here, this effect was negligible and Eq. (4) was accurate to within 0.5%.

Assuming that one is in region B of Fig. 1, the expansion for n_-^2 can be written as

$$n_-^2 \approx \epsilon_L/\epsilon_0 + (Ne/\epsilon_0\omega B)(1+B_r/B), \qquad (5)$$

where $B_r=\omega m^*/e$ is the cyclotron resonant field. Combining Eqs. (4) and (5) yields

$$M^2=\left(\frac{\omega L}{\pi c}\right)^2\frac{\epsilon_L}{\epsilon_0}+\left(\frac{\omega L}{\pi c}\right)^2\frac{Ne}{\epsilon_0\omega B_M}\left(1+\frac{B_r}{B_M}\right), \qquad (6)$$

where B_M denotes the magnetic field value of the Mth reflection minimum. Thus, by fitting the experimental points (B_M,M) to this expression, one can in principle determine ϵ_L, N, and m^*.

It can be seen from Eq. (6) that the relative accuracy with which these parameters are determined depends on the carrier density and available magnetic field range. In order to determine ϵ_L accurately one needs small N or high magnetic fields. In order to determine m^* accurately one must be able to resolve interference structure at low magnetic fields.

When working in the region where the conditions $\omega_c\tau\gg1$ and $\omega_c\gg\omega$ begin to break down, the validity of neglecting higher-order terms can be readily seen by comparison of the largest terms neglected to the terms retained in the expansion. As additional verification that the elementary approach used will provide accurate measurement of the sample parameters as claimed, computer calculations were made for the magnetic field dependence of the reflected microwave power using the exact expressions for n_- and k_- for one type of charge carrier. To make these calculations, the general boundary-value problem for electromagnetic radiation incident on a thin slab was considered. The theoretical results for the reflection coefficient R are well known.[58] The value of every parameter except τ in the equation for R was measured in this experiment making use of the approximations given previously. τ can be determined from the value of the Hall mobility or by considering the envelope of the interference structure as described below.

Figure 2 is a comparison of the theoretical and experimental results for one sample. The theoretical calculations are made at intervals of 0.005 Wb/m² using the values of N, m^*, τ, and ϵ_L determined by these experiments.

B. Inflection-Point Technique

Inspection of the low-field structure of R in Fig. 2 shows that it has the general shape shown in Fig. 3, where we have plotted the absorption coefficient A instead of R. At low fields $A=1-R$ and $T=0$. This shape is described theoretically as arising from cyclotron resonance under skin-effect conditions or nonresonant cyclotron absorption. It was discussed theoretically by Anderson[59] and was mentioned in many of the early papers on cyclotron resonance.[60]

If one uses the experimental technique of magnetic field modulation and phase-sensitive detection, the signal is proportional to dR/dB. This is sketched in Fig. 3 and is seen to have a peak at the inflection point

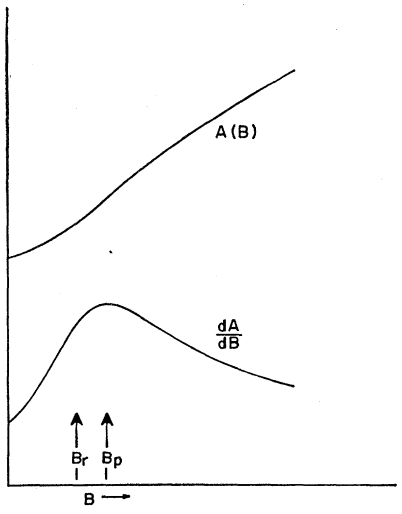

FIG. 3. The low-field microwave absorption coefficient $A=1-R$ and its derivative plotted as functions of magnetic field. $A(B)$ has an inflection point and dA/dB a peak at a field value B_p, which is related to the cyclotron resonant field B_r by Eq. (7).

[57] P. E. Rose, M. T. Taylor, and R. Bowers, Phys. Rev. **127**, 1122 (1962).

[58] J. A. Stratton, *Electromagnetic Theory* (McGraw-Hill Book Co., New York, 1941), p. 505.

[59] P. W. Anderson, Phys. Rev. **100**, 749 (1955).

[60] B. Lax and J. G. Mavroides, Solid State Phys. **11**, 261 (1960).

in $R(B)$. Dexter and Lax[61] showed that this peak occurs at a field position given by

$$B_p = B_r + K/\mu, \tag{7}$$

where $B_r = \omega m^*/e$, μ is the mobility, and K is a parameter of order unity. Thus, if μ is known from Hall measurements or from analysis of the amplitude envelope of the helicon-interference fringes (to be discussed in Sec. II C), and if an accurate value of K is calculated as shown below, then one can obtain m^* from a measurement of B_p at a given microwave frequency. If μ is not known from other sources it may be determined along with m^* from measurement of B_p at two different frequencies by solving Eq. (7) simultaneously at two frequencies.

K may be determined by considering the expression for A:

$$A \approx 1-R = 1-\left|\frac{(n-ik)-1}{(n-ik)+1}\right|^2 = \frac{4n}{(n+1)^2+k^2}. \tag{8}$$

Making the approximations $(n+1)^2 \approx n^2+2n$ and $|(\omega-\omega_c)\tau \operatorname{Im}\epsilon| \gg \epsilon_L$ one obtains an approximate value for the magnetic field at which $d^2A/dB^2=0$, namely, Eq. (7) with

$$K \approx (1/\sqrt{3})[(1-5\eta)/(1-10\eta/3)^{1/2}], \tag{9}$$

where

$$\eta = (2\epsilon_0\omega/\sigma)^{1/2} = (2\epsilon_0\omega/Ne\mu)^{1/2} = (2\omega/\omega_p{}^2\tau)^{1/2}.$$

This expression is plotted in Fig. 4 and gives excellent agreement with computer calculations of the peak of $-dA/dB$.

Figure 5 shows the experimental regimes in which the B_p technique is able to yield m^* and/or μ measurements. When ω_c/ω (which is equivalent to B_p/B_r) is ≈ 2, the mass and mobility are making roughly equal contributions to the position of B_p and can both be determined. This is roughly the central portion of region A. If $\omega\tau$ is too low ($\lesssim 0.06$) one is in region B and B_p is determined almost entirely by μ so that m^* cannot be measured accurately. Above the curved gray border (region C) all the approximations break down and the technique is not applicable.

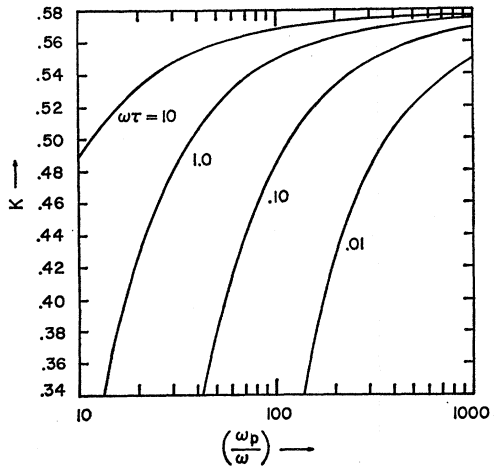

FIG. 4. The parameter K shown as a function of the normalized parameter ω_p/ω for various values of $\omega\tau$.

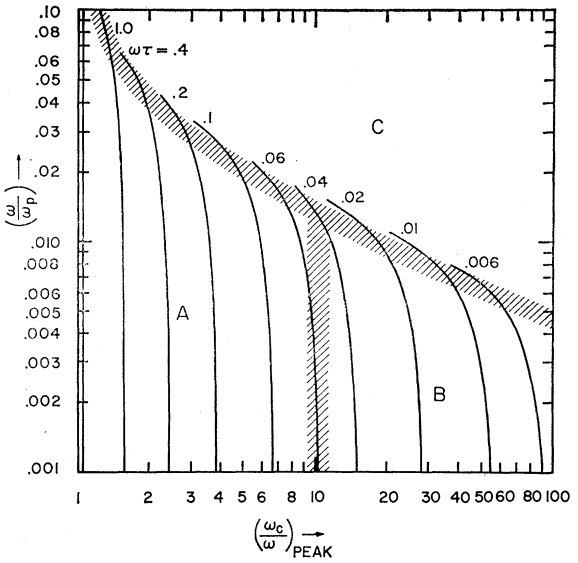

FIG. 5. A diagram for determining the applicability of the inflection-point technique for determining m^* and μ. See explanation in text.

Since this phenomenon occurs at very low fields, its use requires slow, careful field sweeps and accurate low-field calibration. It is also susceptible to interference from microwaves which leak around the sample and are reflected back to interfere with the main signal. This necessitates careful sample mounting. As a final cautionary note it should be emphasized that we have assumed circularly polarized microwaves. Lack of circular polarization means that some of the CRI tail of dA/dB will also be present on the CRA side of B. This tends to shift B_p to higher fields. The theoretical analysis is more difficult for the case of linear polarization but K values may be obtained numerically and are larger than those reported here for circularly polarized microwaves. Thus, in the case of linear polarization, μ plays a larger role in determining B_p and the method becomes less sensitive to m^*. In addition to the shift to higher fields, the peak becomes broader and the sensitivity of the method is further reduced. These effects limit the usefulness of the technique in the case of linear polarization.

C. Analysis of Helicon-Interference Envelope

In this section it will be shown that the carrier mobility can be determined from a relatively simple analysis of the amplitude envelope of the helicon-interference structure. This measurement of μ can be

[61] R. N. Dexter and B. Lax, Phys. Rev. **100**, 1216 (1955).

combined with the inflection point at B_p to obtain m^* without the necessity of measuring B_p at two frequencies (see Sec. II B). Thus, in principle, one can obtain N, m^* (two ways), ϵ_L/ϵ_0, and μ from one experimental trace.

In the helicon approximation, interference of first surface reflection with waves that make one round-trip pass through the sample will cause a relative deviation Δ_1 from the intensity of the first surface reflection, which is approximately given by

$$\ln(\Delta_1/B)\approx C_1-C_2B^{-3/2}, \tag{10}$$

where C_1 is unimportant and C_2 is given by

$$C_2=(\omega NeL^2/\epsilon_0c^2)^{1/2}\mu^{-1}. \tag{11}$$

Thus, a plot of $\ln(\Delta_1/B)$ versus $B^{-3/2}$ for several values of B gives a straight line with a slope proportional to μ^{-1}. The proportionality constant is known since N is measured from the helicon-interference-fringe analysis.

The envelope of dR/dB (which is recorded easily by use of field modulation and phase-sensitive detection) is experimentally easier to determine and equally amenable to analysis. The deviation Δ_2 of dR/dB from the background slope due to first surface reflection is given approximately by

$$\ln(\Delta_2B^{1/2})\approx C_3-C_2B^{-3/2}, \tag{12}$$

where C_2 is again given by Eq. (11).

The above expressions are useful only in the low-field portion of the interference fringes where the envelope is opening up. At higher fields the failure of our two-term interference assumption and the addition of extra damping mechanisms cause the envelope to turn over and begin closing. When this begins to happen Eqs. (10) and (12) are no longer valid. Furdyna[56] has discussed the effect of the hole plasma on the damping envelope at higher magnetic fields.

Use of Eq. (12) with computer-generated data and with experimental traces of dR/dB confirms the value of the technique. For samples with $N\approx10^{21}$ m^{-3} the results were within 10% of the known values. For samples of higher carrier density the approximations are better satisfied and the results are correspondingly better.

Stradling[62] has discussed another method of using the low-field reflection coefficient but we feel that the inflection-point method is simpler and more accurate.

III. EXPERIMENTAL

Helicon propagation in InSb was investigated at microwave frequencies of 9, 24, and 70 GHz. The microwave systems were conventional with klystron stabilization to the cavity frequency or to the peak power in nonresonant waveguide units. The systems were mounted in a double Dewar unit with both internal and external field-modulation coils which were usually driven at 500 Hz. Coherent detection was utilized in order to record dR/dB; when we wished to record a signal proportional to the reflectivity we connected the crystal detector to an x-y recorder through an impedance matching unit. Most experiments were performed with microwave spectrometers which utilized circularly polarized microwaves that were produced in the Galt configuration.[63] Microwaves passed down one arm of a U-shaped waveguide from which they were coupled into a cylindrical cavity resonant in the TE_{113} mode. The specimen, usually in the form of a thin slab, was placed outside the back wall of the resonant cavity to which it was coupled by a small iris in the center of the back wall. The back wall itself was removable and studies were made of the effect of the iris diameter and wall thickness. Coupling the microwaves through an iris in this manner should be expected to introduce a phase shift which depends on the thickness of the cavity wall and the iris diameter, as well as the phase and amplitude of the wave reflected from the sample surfaces back into the cavity. This phase shift is, in principle, a function of magnetic field and can be very troublesome in the analysis. It is frequently possible, however, to assume that the phase shift δ is independent of B. The interference condition is then modified in such a way that Eq. (6) becomes

$$(M-\delta)^2=\left(\frac{\omega L}{\pi c}\right)^2\frac{\epsilon_L}{\epsilon_0}+\frac{Ne}{\epsilon_0\omega B_M}\left(\frac{\omega L}{\pi c}\right)^2\left(1+\frac{B_r}{B_M}\right). \tag{13}$$

In nearly all cases we are able to fit our data with this expression, determining δ as a physically uninteresting fourth parameter.

The signal reflected from the sample was detected by a crystal detector located on the output arm of the waveguide. With this configuration excellent circular polarization could be established for the microwaves incident on the sample, and the propagation vector of the microwaves could be adjusted to any angle relative to the dc magnetic field. The transmitted signal was also detected in these experiments. This was done by placing a waveguide pickup immediately behind the sample and conducting the signal to a crystal detector located outside the Dewar system. Extreme care was taken to insure that there was no leakage of microwaves around the sample to the waveguide pickup and no metallic contact with the sample surface. In general, the admixture of microwaves which have not passed through the sample and microwaves transmitted through the sample causes severe complications in the resulting signal. In the best experimental conditions this reduces to a doubling of the peaks.[5] The reason for taking precautions to prevent the sample from making electrical contact with a conductor was to prevent the propagation of electromagnetic waves on the sample

[62] R. A. Stradling, Proc. Phys. Soc. (London) **90**, 175 (1967).

[63] J. K. Galt, W. A. Yager, F. R. Merritt, B. B. Cetlin, and A. D. Brailsford, Phys. Rev. **114**, 1396 (1959).

surface.[53,64] These surface waves are a common nuisance in the determination of semiconductor parameters.

In the Introduction we discussed some of the advantages of observing the reflected signal. The cavity methods permit good contrast, high sensitivity, small specimens, and convenient horizontal geometry. Our configuration also permitted transmission studies of the Fabry-Perot[43] and Rayleigh[56] types. All waveguide and cavity configurations were sensitive to artifacts in the low-transmission region, as we point out in several places in this paper. The ease of establishing a circularly polarized wave propagating in the horizontal direction was the primary experimental consideration which led us to favor the Galt configuration. Similar results were obtained in the waveguide experiments.

Helicon propagation was studied in n-type samples of InSb with electron concentrations ranging from 8×10^{19} to 6.7×10^{22} m^{-3} at 77°K and in one sample which was p type at this temperature. Helicon effects were studied from temperatures of 77 to 300°K in magnetic fields up to 1.1 or in some cases 1.9 Wb/m^2 provided by a Varian 12-in. electromagnet. The samples were also surveyed at liquid-helium temperatures but the carrier concentration had become so low[65] that interference structure of helicon propagation was not observed at these temperatures. The dependence of helicon propagation on frequency and sample geometry was also studied. Section IV describes our procedure for analyzing these data and the experimental results.

IV. ANALYSIS OF DATA AND OBSERVATIONS

From a typical experimental trace of dR/dB, such as Fig. 6, we would first obtain the values of B_M which correspond to interference maxima. These permit a determination of N, m^*, and ϵ_L from Eqs. (6) or (13). Having determined the carrier density, one can analyze

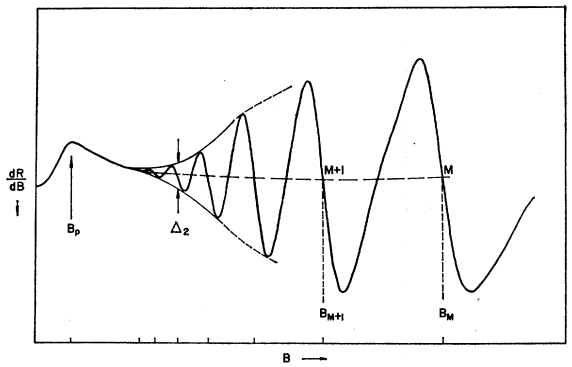

FIG. 6. A photograph of an experimental curve which illustrates the sources of our experimental data. The low-field peak B_p, the opening part of the amplitude envelope, Δ_2, and the field positions of the interference fringes, B_M, contain useful and partially redundant information about N, m^*, μ, and ϵ_L.

[64] H. Toda, J. Phys. Soc. Japan **19**, 1126 (1964).
[65] H. J. Hrostowski, F. J. Morin, T. H. Geballe, and G. H. Wheatley, Phys. Rev. **100**, 1972 (1955).

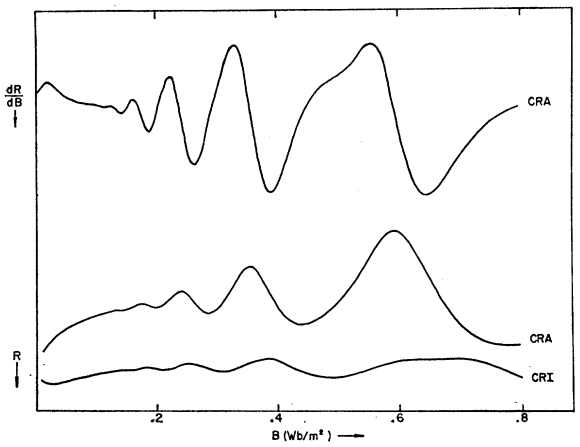

FIG. 7. Experimental traces taken at 23 GHz and 77°K showing the reflected signal and its derivative for the CRA side of B and showing the reflected signal on the CRI side of B. This structure on the CRI side is attributed to a surface mode of propagation.

the amplitude envelope using Eqs. (11) and (12) to obtain μ. Finally, one may use N and μ to obtain m^* from the low-field inflection point and Eq. (7), using Eq. (9) to obtain K.

Helicon propagation was observed in single-crystal specimens of InSb ranging in thickness from 1.0 to 6.5 mm with similar effects observed in all samples investigated. Detailed studies were then performed on several specimens chosen with appropriate carrier concentrations and thicknesses such that several interference maxima were observed at frequencies of 70 and 24 GHz. These specimens were then studied to determine the values of N, m^*, ϵ_L, and μ. Sample C_L will be used as an example despite its relatively low carrier concentration of 8×10^{20} m^{-3}. As explained in Sec. II C this makes it a poor candidate for determining μ from amplitude analysis at 70 GHz. Moreover, its Hall mobility of 36 m^2/V sec is too low for a good determination of m^* with 24-GHz microwaves since $\omega\tau=0.43$. Thus, its marginal location with respect to the optimum experimental regimes affords an opportunity to observe the breakdown of the approximations used in the simplified theory of the effects. In spite of this fact, successful amplitude analyses, m^* and N determinations were made, as discussed below. With samples of higher carrier density, all approximations improve but it is no longer possible to determine the lattice dielectric constant at the low magnetic fields utilized in our experiments.

Figure 7 is a photograph of data taken at 77°K using circularly polarized microwaves of frequency 24 GHz incident on a specimen of 1.64-mm thickness. Figure 8 shows data taken on the same specimen and at the same temperature but at a microwave frequency of 70 GHz. The experimental regime for Fig. 8 is the B region of Fig. 1. Thus, B_r/B_M is significant in Eq. (6) and the effective mass is easily determined. The measured B_r in

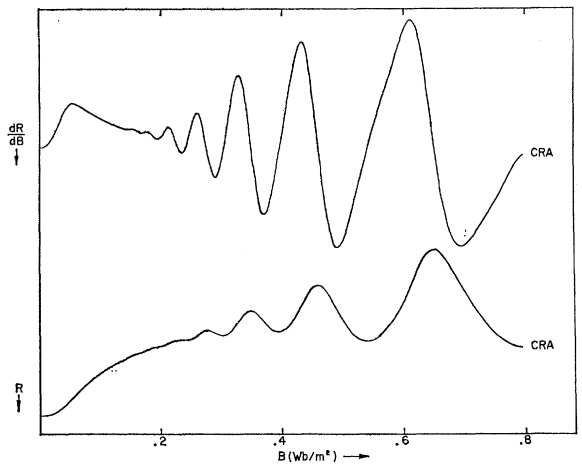

FIG. 8. Experimental traces taken at 70 GHz and 77°K showing the reflected signal and its derivative on the CRA side of B.

our experiments consistently yielded a value for the electronic effective mass of $m^*=0.014\,m_0$. The experimental regime of Fig. 7 is region C of Fig. 1 and m^* is not easily obtained from the helicon propagation. On the other hand, amplitude analysis gives μ, which in combination with N gives an accurate measurement of m^* from the value of B_p, the inflection point. Measurements of ϵ_L/ϵ_0 in these experiments yielded an average value of 19.7 ± 0.5

Figures 7 and 8 permit a demonstration of the two-frequency inflection-point technique. For this sample, helicon measurements give $N=8.4\times10^{20}$ m^{-3}, $\epsilon_L/\epsilon_0=20$, $m^*/m_0=0.014$, and a Hall measurement gave $\mu=36$ m$^2/V$ sec. Table I shows the results of the B_p measurements, which are in excellent agreement with the helicon and Hall results and are taken as mutual confirmation of the reliability of these techniques.

The inflection-point technique can be used even in cases where the helicon results are in doubt due to inability to resolve fringes at low enough fields to make B_T/B_M significant, or low $\omega\tau$. Caution should be used, however, when mass values are obtained *exclusively* from B_p measurements. Various artifacts in the low-field reflection coefficient, including the phase shift δ mentioned in Sec. II A, can lead to erroneous results.

Table II shows the semiconductor parameters that could be determined from two traces such as dR/dB of Figs. 7 and 8. Hall effect and conductivity results are included for comparison. It should be noted that the Hall effect yields an average carrier density for the specimen, whereas the microwave techniques sample only that region directly in line with the coupling iris. The carrier density is in all cases the parameter best determined by the helicon propagation.

TABLE I. Measured values of the low-field inflection point B_p in the microwave reflection coefficient are given for two frequencies. These values, together with the corresponding K values from Eq. (9), are used to calculate m^* and μ.

Measured frequency (GHz)	Measured B_p (Wb/m²)	K value using Eq. (28)	Results
70.63	0.0499	0.495	$m^*/m_0=0.0141\pm0.0007$
23.74	0.0267	0.530	and $\mu=37\pm7$ m²/V sec

TABLE II. Summary of the full set of semiconductor parameters which could be determined from two traces such as dR/dB of Figs. 7 and 8 including our experimental results for InSb sample C_L. Hall effect and conductivity results are included for comparison.

Method	$N(m^{-3})$ 10^{20}	m^*/m_0	μ(m²/V sec)	ϵ_L/ϵ_0
Interferometry at 23 GHz	8.41	0.0145±0.0015	···	18 ±5
Amplitude analysis at 23 GHz	···	···	40±5	···
Inflection point using μ from 23-GHz amplitude analysis	···	0.0159±0.002	···	···
Interferometry at 70 GHz	8.36	0.0140±0.0005	···	19.7±5
Amplitude analysis at 70 GHz	···	···	31±5	···
Inflection point using μ from 70-GHz amplitude analysis	···	0.0135±0.001	···	···
Inflection-point technique using two frequencies	···	0.0141±0.0007	37±7	···
Hall effect and conductivity	8.6	···	36±1	···

V. SUMMARY

We have made a detailed study of helicon propagation in InSb at microwave frequencies and have measured the index of refraction in a magnetic field by observing the geometric resonances associated with helicon propagation.

In the course of our helicon studies we also found that the low-field inflection point in $R(B)$ could be exploited quantitatively to provide an independent measure of m^* and μ. The helicon and inflection-point techniques complement each other in the following sense. The helicons yield an N value and μ estimate necessary for the interpretation of B_p and the inflection-point technique provides an accurate m^* in cases where the helicon analysis is difficult or the resolution of interference fringes is poor. In the limit of no interference fringes at all, the inflection-point technique could be combined with Hall measurements to give m^*.

We have studied helicon effects in InSb primarily to determine their usefulness in semiconductors for measuring the effective mass of the charge carriers supporting the helicon mode of propagation. It was, of course, well known that helicon effects could be used to measure the free-electron density and the lattice dielectric constant. The energy gap may be determined through studies of the temperature dependence of the carrier concentration as in Hall-effect studies. We have

concluded that the helicon phenomena and nonresonant cyclotron absorption can be used to make rapid and accurate measurements of the electron concentration, the effective mass, the Hall mobility, and the lattice dielectric constant. Comparison of measured values with literature values or the results of Hall and conductivity studies confirmed the validity of these techniques of experiment and analysis. We have summarized the attractive experimental regimes in the form of charts plotted in terms of the natural frequencies, ω, ω_c, ω_p, and $1/\tau$.

Although our presentation is specifically for isotropic materials with spherical constant-energy surfaces, many of these results can be generalized[32] for studying band-structure effects in anisotropic materials. In a significant group of semiconductors, however, our assumptions are well fulfilled and the analysis described above has been utilized successfully for band studies in the alloy system $Hg_{1-x}Cd_xTe$, as well as in gray tin. The techniques are applicable to a number of other semiconducting alloys and compounds. Since the techniques reported here allow the *simultaneous* measurement of N, μ, and m^*, they are very attractive for transport studies of these parameters as functions of temperature.

ACKNOWLEDGMENTS

We wish to thank Dr. G. R. Cronin of Texas Instruments Corp. for providing several InSb specimens. We also thank P. L. Radoff for his assistance with some of the experiments.

PHYSICAL REVIEW VOLUME 181, NUMBER 3 15 MAY 1969

Helicons and Nonresonant Cyclotron Absorption in Semiconductors. II. $Hg_{1-x}Cd_xTe$†‡

JOHN D. WILEY* AND R. N. DEXTER
Department of Physics, University of Wisconsin, Madison, Wisconsin 53706
(Received 25 September 1968)

We have used microwave helicons of 23 and 70 GHz and nonresonant cyclotron absorption to measure the carrier densities, effective masses, and mobilities of electrons in $Hg_{1-x}Cd_xTe$ for $0.135 \leq x \leq 0.203$. Most measurements were made at 77°K, but some values are reported for 1.3°K. Carrier concentrations at 77°K ranged from 8×10^{20} to 2×10^{22}m^{-3} and were sufficiently low to enable us to measure m^* close to the conduction-band edge. The mass values, in the range $0.004m_0$–$0.010m_0$, are in good agreement with values calculated from Kane's expression for the conduction band using literature values for the energy gap, its variation with temperature and alloy concentration, and the momentum matrix element, P. One specimen with $x=0.149$ was studied from 77 to 185°K. Over this range the mobility was closely proportional to T^{-2}. The variation of electron density permitted an estimate of the effective mass of the holes, $m_h^*=0.71m_0$.

I. INTRODUCTION

IN the preceding paper[1] (hereafter referred to as I), we described microwave techniques for making simultaneous measurements of carrier concentration N, effective mass m^*, and mobility μ in certain classes of semiconductors. These experimental techniques, helicon propagation and nonresonant cyclotron absorption (NRCA), have been used to study several samples of the alloy $Hg_{1-x}Cd_xTe$ in the neighborhood of $x=0.15$, where the Γ_6-Γ_8 energy gap goes through zero in a transition from semimetallic to semiconducting behavior. The small energy gaps at 77°K for samples with $0.08<x<0.20$ lead to extremely small electronic effective masses and strongly nonparabolic conduction bands. Due to band filling, the effective mass is a strong function of the carrier concentration. Thus, simultaneous measurements of N and m^* are ideal for studying the conduction band in $Hg_{1-x}Cd_xTe$.

It is well established[2–11] that the nonparabolicity of

† Sponsored by the Aerospace Research Laboratories, Office of Aerospace Research, U. S. Air Force.

‡ This paper is based on portions of a thesis submitted by J. D. W. in partial fulfillment of the requirements for the Ph.D. degree at the University of Wisconsin.

* Present address: Bell Telephone Laboratories, Murray Hill, N. J.

[1] John D. Wiley, P. S. Peercy, and R. N. Dexter, preceding paper, Phys. Rev. 181, 1173 (1969).

[2] T. C. Harman, A. J. Strauss, D. H. Dickey, M. S. Dresselhaus, G. B. Wright, and J. G. Mavroides, Phys. Rev. Letters 7, 403 (1961).

[3] A. J. Strauss, T. C. Harman, J. G. Mavroides, D. H. Dickey, and M. S. Dresselhaus, in *Proceedings of the International Conference on the Physics of Semiconductors, Exeter* (The Institute of Physics and the Physical Society, London, 1962), p. 703.

[4] R. Piotrzkowski, S. Porowski, Z. Dziuba, J. Ginter, W. Giriat, and L. Sosnowski, Phys. Status Solidi 8, K135 (1965).

[5] C. Verié and E. Decamps, Phys. Status Solidi 9, 797 (1965).

[6] W. Szymanska, L. Sniadower, and W. Giriat, Phys. Status Solidi 10, K11 (1965).

[7] M. Mali, Phys. Status Solidi 13, 215 (1966).

[8] W. Szymanska, Phys. Status Solidi 23, 69 (1967).

[9] W. Giriat, in *Proceedings of the International Conference on II–VI Semiconducting Compounds, Providence, 1967*, edited by D. G. Thomas (W. A. Benjamin, Inc., New York, 1968), p. 1058.

[10] R. R. Galazka and L. Sosnowski, Phys. Status Solidi 20, 113 (1967).

[11] L. Sosnowski and R. R. Galazka, in *Proceedings of the International Conference on II–VI Semiconducting Compounds, Providence, 1967*, edited by D. G. Thomas (W. A. Benjamin, Inc., New York, 1968), p. 888.